

# Complete $^1\text{H}$ and $^{13}\text{C}$ NMR signal assignments and chemical shift calculations of four 1,2,4-oxadiazole-based light-emitting liquid crystals

Ricardo O. Silva · Ricardo A. W. Neves Filho ·  
Rodrigo Azevedo · Rajendra M. Srivastava ·  
Hugo Gallardo

Received: 11 August 2009 / Accepted: 18 December 2009 / Published online: 13 January 2010  
© Springer Science+Business Media, LLC 2010

**Abstract** In this article, we describe the complete  $^1\text{H}$  and  $^{13}\text{C}$  NMR signal assignments of four 1,2,4-oxadiazoles possessing light-emitting liquid crystal properties. These results were obtained by using one- and two-dimensional NMR techniques as well as GIAO (PCM) calculations at B3LYP/6-311++G(d,p) level for compounds **1** and **2a–d**. The computed values are in good agreement with the ones obtained experimentally. In addition, some previously unexplained thermotropic features of compounds **2a–d** could be clarified with the help of the geometry optimization calculations carried out by us.

**Keywords** Liquid crystals · 1,2,4-Oxadiazole · Spectroscopy · Chemical shift calculations

## Introduction

Luminescent organic compounds have been attracting continuous attention for the last two decades due to their exciting applications in a large number of electron-optical devices [1–5]. Currently, the use of such substances as organic light-emitting diodes (OLEDs) has been the focus of academic as well as industrial research groups, because OLEDs have certain advantages over liquid crystal display

(LCD) technology [1, 6–8]. Among organic compounds, highly  $\pi$ -conjugated molecules containing electron-deficient heterocyclic rings have shown specific advantages due to their abilities in transporting electrons [1, 7–16].

The foregoing observations for such compounds are particularly noteworthy, and we have already devoted efforts in synthesizing and characterizing thermally stable luminescent liquid crystals possessing 1,2,3-triazole [17], 2,1,3-benzothiadiazole [18], isoxazole [19], and 1,2,4- or 1,3,4-oxadiazole moiety in their molecular frameworks [20–23].

In general, the structure assignments of these valuable compounds have been made by simply analyzing the infrared and NMR spectral data. Although the signal assignments in the NMR spectra seem reasonable, they are based mostly on the guesswork and sometimes utilizing similar data available in the literature but without confirmation by other spectral techniques.

In practice, the calculations involving nuclear magnetic shielding are quite useful for signal assignments because when they are compared with the shielding of the reference compound, their chemical shifts can be predicted [24–26]. In fact, while employing either the ab initio or DFT calculations incorporated with GIAO, which furnish the chemical shift values much better and are closer to the experimental values. [27]. This kind of approach was successfully applied for 1,2-oxathianes [28], aziridines [29], calix[4]arenes [30], and heterocyclic compounds [31]. In general, chemical shift calculations of these latter systems are more difficult to achieve because of the presence of hetero-aromaticity and tautomerisms, which are complicated to describe computationally. Therefore, methods based upon the density function theory (DFT) are more desirable since DFT approach includes electronic correlation as well as relativistic effects [31]. Besides this, DFT method also needs relatively lower

R. O. Silva · R. A. W. Neves Filho · R. Azevedo ·  
R. M. Srivastava (✉)  
Departamento de Química Fundamental, Universidade Federal  
de Pernambuco, Recife, PE 50.740-540, Brazil  
e-mail: rms\_indu@yahoo.com; rms@ufpe.br

R. A. W. Neves Filho · H. Gallardo  
Departamento de Química, Universidade Federal de Santa  
Catarina, Florianópolis, SC, Brazil

computational demand in comparison with the MP2 approach [31].

Our literature search revealed that no effort has been made to make the correct assignments of the proton and carbon signals for the luminescent substances containing 1,2,4- and 1,3,4-oxadiazole moieties. As we recently detected the unusual properties of a series of highly birefringent 1,2,4-oxadiazole-based blue fluorescent liquid crystals **2a–d**, we decided to reexamine the  $^1\text{H}$  and  $^{13}\text{C}$  NMR signal assignments of four just-cited compounds to make the unambiguous assignments. In order to achieve this goal, additional complementary NMR techniques (not used earlier) and chemical shift calculations using DFT-GIAO approach have been performed. These NMR techniques are: distortionless enhancement by polarization transfer (DEPT), correlation spectroscopy (COSY), heteronuclear multiple bond connectivity (HMBC), heteronuclear multiple quantum coherence (HMQC), and nuclear Overhauser effect spectroscopy (NOESY) methods which in conjunction with computational calculations provided us with the correct assignments of all the protons as well as carbons' nuclei for the above mentioned compounds (Fig. 1).

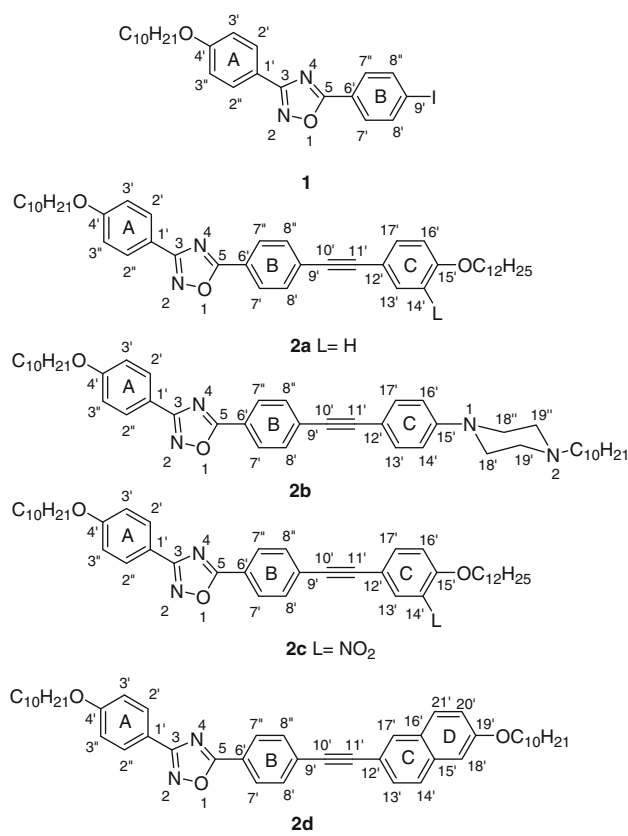


**Fig. 1** Compounds analyzed in this study

## Experimental

Compounds **1** and **2a–d** have been synthesized as described earlier by our research group [21].

The NMR spectra of all compounds were obtained on a Varian Unity Plus (7.04 T) spectrometer operating at 300 and 75.4 MHz for  $^1\text{H}$  and  $^{13}\text{C}$  nuclei, respectively. Compounds **2a–d** have been dissolved in  $\text{CDCl}_3$ , and the residual solvent signal at  $\delta$  7.26 ppm has been used as an internal chemical shift reference for the protons.  $^1\text{H}$  NMR spectra were obtained using 16 transients, acquisition time 3.7 s, and pulse width of 8  $\mu\text{s}$  ( $45^\circ$  pulse), whereas  $^{13}\text{C}$  NMR spectra were measured using 1800 transients, acquisition time 1.0 s, and pulse width of 4  $\mu\text{s}$  ( $30^\circ$  pulse). Bidimensional spectra were acquired without spinning the samples.

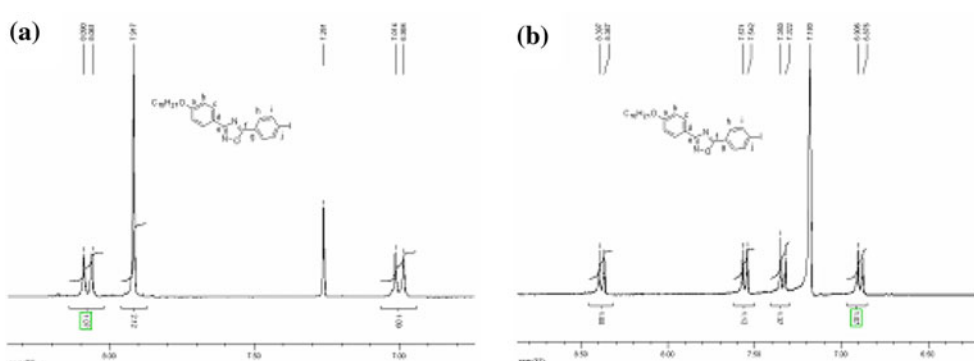
Molecular orbital calculations have been carried out using Gaussian 03 program [32]. In our calculations, we have used a propyloxy chain instead of decyloxy group attached at the phenyl ring to diminish the computational time demand. The geometry optimization for compound **1** has been achieved by employing HF/6-31G(d) method for H, C, O, and N atoms and SDD basis set including SDD pseudo-potential for iodine atom. Chemical shift calculations of compound **1** have been carried out at B3LYP level by using 6-311++G(d,p) for C,H,O, and N atoms, and SDD for iodine atom. For geometry optimization of compounds **2a–d**, the HF/6-31G(d) has been employed. The chemical shift calculations for compounds **2a–d** have been carried out at B3LYP/6-311++G(d,p) level of theory using TMS B3LYP/6-311++G(d,p) GIAO as reference. In both cases, the solvent effects have been considered employing polarizable continuum model (PCM).

## Results and discussion

### $^1\text{H}$ and $^{13}\text{C}$ nuclear magnetic resonance assignments

First, we decided to analyze compound **1** because this is the key intermediate for obtaining substances **2a–d**. The signal assignments of this compound would help in general although it does not exhibit either mesomorphism or luminescence. Initially, we examined the  $^1\text{H}$  NMR spectrum of **1** in  $\text{CDCl}_3$  which showed three signals at  $\delta$  7.00, 7.91, and 8.07 ppm, respectively. Here, the former and the latter signals appeared as doublets ( $J = 9.0$  Hz, AA'BB' system). The first signal is due to H-3' and H-3'', and the second belongs to H-2' and H-2''. COSY NMR technique supported this observation. Surprisingly, the signal at  $\delta$  7.91 ppm integrated for four protons and appeared as a singlet. Since, we already established the chemical shifts of H-2', H-2'', H-3', and H3'', the singlet at  $\delta$  7.91 ppm, (4H)

**Fig. 2** **a** Aromatic region of  $^1\text{H}$  NMR spectrum of compound **1** in  $\text{CDCl}_3$ , **b** Aromatic region of  $^1\text{H}$  NMR spectrum of compound **1** in benzene- $d_6$



must be due to the other phenyl ring containing the iodine atom.

When the spectrum of **1** was obtained in benzene- $d_6$ , the singlet at  $\delta$  7.91 ppm separated into two doublets (AA'BB' system,  $J = 8.6$  Hz)—one at  $\delta$  7.33 ppm and the other at  $\delta$  7.56 ppm, respectively. This phenomenon is certainly due to anisotropic effect of the solvent. These signals are due to H-7' and H-7'', and H-8' and H-8'' nuclei, respectively. This way, the complete assignment of all  $^1\text{H}$  NMR signals has been made for compound **1** (Fig. 2).

When the iodine atom was substituted with *p*-alkyloxyphenylethyynyl group (**2a**), there was a little change in ring “A”. The protons of rings “B” and “C” appeared as two sets of doublets of doublets (dd, AA'BB' system). For ring “B”, there were two doublets—one at  $\delta$  7.65 ppm, representing H-8' and H-8'' nuclei, and the other signal at  $\delta$  8.20 ppm belonging to H-7' and H-7'' nuclei, respectively. The protons of ring “C” appeared at  $\delta$  6.8 ppm (d, 2H, H-14', and H-16') and the other at  $\delta$  7.5 ppm (d, 2H, H-13', and H-17'). The spectrum of HMQC correlated the carbon signals which appeared at their appropriate positions (Fig. 3).

HMQC experiment confirmed the position of C-4' at  $\delta$  161.5 ppm, and the other quaternary carbon C-15' at  $\delta$  159.7 ppm (see Table 1). Similarly, the same experiment

correlated H-8' with C-10' (at  $\delta$  87.3 ppm) and H-17' with C-11' (at  $\delta$  93.2 ppm), respectively. Thus, the identity of all the signals have been accounted for.

Next, we turned our attention on compound **2b**, where the alkoxy group attached on ring “C” was replaced with *N,N'*-disubstituted piperazine ring. For the *N,N'*-disubstituted piperazine ring, we had three sets of protons between  $\delta$  2.50 and 3.40 ppm—one at  $\delta$  2.48 ppm (m, 2H) and the others at  $\delta$  2.71 ppm (dd, 4H) and at  $\delta$  3.36 ppm (dd, 4H). Here, we faced the challenge for recognizing their appropriate positions. The first one at  $\delta$  2.48 ppm was easy to attribute because the COSY spectrum clearly indicated that this methylene group had coupling with the other  $-\text{CH}_2-$  protons linked to it. Therefore, this  $\text{CH}_2$  is attached to the N-2 atom of the piperazine ring.

The two sets of methylene protons of the piperazine ring needed more thorough study for their correct attribution. Since we already had established the correct location of H-14' and H-16' at  $\delta$  6.87 ppm, it was possible to see that both these protons produced the nuclear Overhauser effect on the methylene protons linked with N-1, when the signal at  $\delta$  6.87 ppm was irradiated; this was also supported by NOESY spectrum. Therefore, the other four protons of the  $\text{CH}_2$  group of the piperazine ring are at  $\delta$  3.36 ppm (Fig. 4).

When the hydrogen atom at 14' in **2c** was replaced with a nitro group, there was no change in the chemical shift of the protons of rings “A” and “B”. As expected, the major change occurred in ring “C” protons. The H-13' signal moved downfield and appeared at  $\delta$  8.01 ppm as a singlet; the H-16' signal also shifted downfield by 0.16 Hz and presented a clear doublet at  $\delta$  7.04 ppm ( $J = 9.0$  Hz); the H-17' had a similar behavior but was superimposed with the doublet of H-8' and H-8'', which was not separable in the  $^1\text{H}$  NMR spectrum. However, the HMQC bidimensional examination clearly indicated that H-17' is attached to carbon atoms C-17', whereas C-8' and C-8'' are connected to H-8' and H-8'', respectively. Thus, we have been able to establish the identities of all the hydrogen and carbon atoms of the entire molecule (Fig. 5).

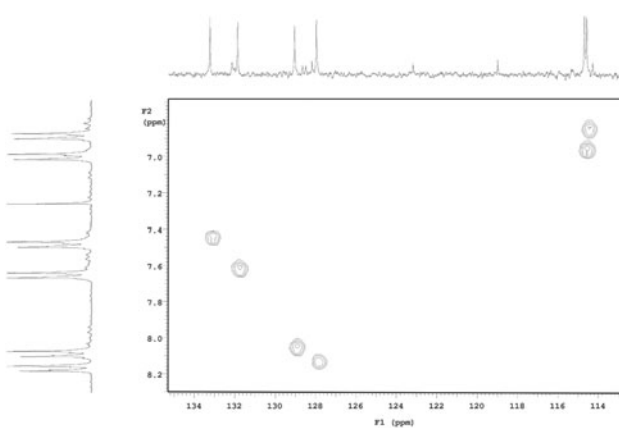


**Fig. 3** Expansion of HMQC spectrum of compound **2a**

**Table 1** Experimental and calculated values of  $^1\text{H}$  and  $^{13}\text{C}$  chemical shifts for compounds **1–2**

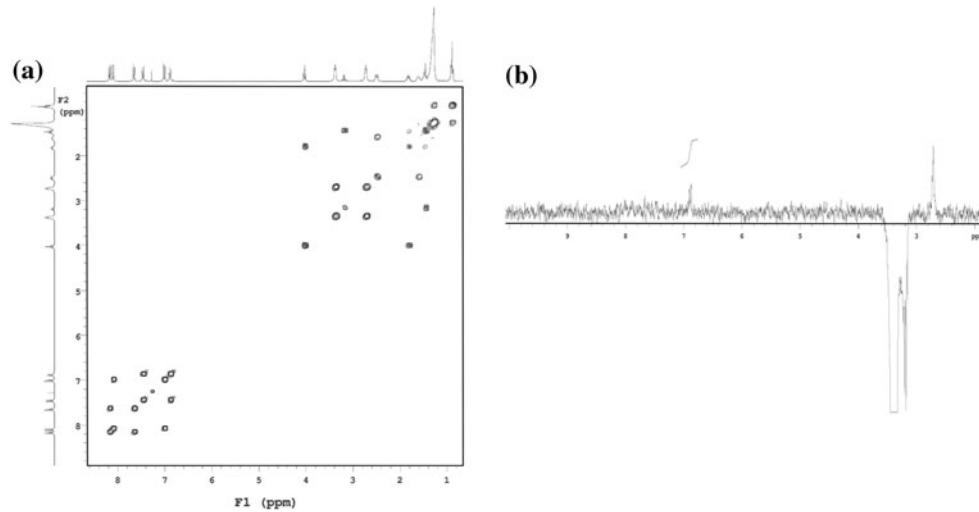
$^1\text{H}$ or $^{13}\text{C}$ location	Compound <b>1</b> ( $\text{CDCl}_3$ )				Compound <b>1</b> ( $\text{C}_6\text{D}_6$ )			
	$\delta_{\text{H}}$ - $J$ (Hz) (Exp.)	$\delta_{\text{H}}$ (Calc.)	$\delta_{\text{C}}$ (Exp.)	$\delta_{\text{C}}$ (Calc.)	$\delta_{\text{H}}$ - $J$ (Hz) (Exp.)	$\delta_{\text{H}}$ (Calc.)	$\delta_{\text{C}}$ (Exp.)	$\delta_{\text{C}}$ (Calc.)
3	—	—	168.8	170.2	—	—	—	—
5	—	—	174.7	174.4	—	—	—	—
1'	—	—	118.8	123.4	—	—	—	—
2'/2''	8.07 ( <i>d</i> , 9.0)	8.38	129.1	133.2	8.38	8.34	—	—
3'/3''	6.99 ( <i>d</i> , 9.0)	6.94	114.7	116.5	6.91	6.84	—	—
4'	—	—	161.6	166.6	—	—	—	—
6'	—	—	123.8	129.0	—	—	—	—
7'/7''	7.91 ( <i>s</i> )	8.21	129.4	132.6	7.46	8.15	—	—
8'/8''	7.91 ( <i>s</i> )	7.13	138.4	139.9	7.33	7.03	—	—
9'	—	—	100.0	151.6	—	—	—	—
$\text{CH}_3$	0.89 ( <i>t</i> , 6.6)	0.86	14.1	8.9	0.95	0.85	—	—
$[\text{OCH}_2]$	4.03 ( <i>t</i> , 6.6)	3.52	68.1	68.8	3.58	3.46	—	—
$[\text{CH}_2]$	1.0–2.0	—	22.0–32.0	—	1.0–2.0	—	—	—
$R^2$	0.9895		0.9498 <sup>a</sup>		0.9937		—	
SD	0.49		15.31 <sup>a</sup>		0.37		—	
$^1\text{H}$ or $^{13}\text{C}$ location	Compound <b>2a</b> ( $\text{CDCl}_3$ )				Compound <b>2b</b> ( $\text{CDCl}_3$ )			
	$\delta_{\text{H}}$ - $J$ (Hz) (Exp.)	$\delta_{\text{H}}$ (Calc.)	$\delta_{\text{C}}$ (Exp.)	$\delta_{\text{C}}$ (Calc.)	$\delta_{\text{H}}$ - $J$ (Hz) (Exp.)	$\delta_{\text{H}}$ (Calc.)	$\delta_{\text{C}}$ (Exp.)	$\delta_{\text{C}}$ (Calc.)
3	—	—	168.7	176.7	—	—	168.7	170.4
5	—	—	174.9	188.4	—	—	174.9	175.4
1'	—	—	119.0	127.7	—	—	119.0	123.1
2'/2''	8.09 ( <i>d</i> , 8.7)	8.75	129.1	136.6	8.08 ( <i>d</i> , 8.7)	8.39	129.0	133.7
3'/3''	7.00 ( <i>d</i> , 8.7)	7.76	114.7	122.1	6.99 ( <i>d</i> , 8.7)	7.08	114.7	116.6
4'	—	—	161.5	170.9	—	—	161.5	166.1
6'	—	—	123.2	127.9	—	—	123.0	127.9
7'/7''	8.20 ( <i>d</i> , 8.7)	8.58	128.0	133.8	8.15 ( <i>d</i> , 8.7)	8.45	127.9	131.8
8'/8''	7.65 ( <i>d</i> , 8.7)	7.89	131.9	136.6	7.63 ( <i>d</i> , 8.7)	7.81	131.8	135.5
9'	—	—	128.2	132.8	—	—	128.4	132.8
10'	—	—	87.3	93.3	—	—	87.3	93.1
11'	—	—	93.2	100.3	—	—	93.7	100.3
12'	—	—	114.3	120.1	—	—	112.5	117.3
13'	—	—	—	—	—	—	—	—
14'	—	—	—	—	—	—	—	—
15'	—	—	159.7	168.3	—	—	150.9	161.0
16'	6.80 ( <i>d</i> , 8.7)	7.73	114.6	121.7	6.87 ( <i>d</i> , 8.7)	7.10	115.0	123.3
17'	7.50 ( <i>d</i> , 8.7)	7.99	133.2	140.7	7.44 ( <i>d</i> , 8.7)	7.63	132.9	137.2
$\text{CH}_3$	0.88 ( <i>t</i> , 6.6)	1.13	14.1	15.2	0.88 ( <i>t</i> , 7.2)	0.76	14.1	6.8
$[\text{OCH}_2]$	3.97/4.02 ( <i>t</i> , 6.6)	4.14/4.15	68.1	79.2	4.01 ( <i>t</i> , 6.6)	3.62	68.1	68.4
$[\text{CH}_2]$	1.0–2.0	—	22–32	—	1.0–2.0	—	22.0–32.0	—
$[\text{NCH}_2]$	—	—	—	—	2.48 ( <i>dd</i> , 8.1, 7.8)	2.77	58.7	53.3
$\text{CH}_2\text{--N(1)}$	—	—	—	—	3.36 ( <i>dd</i> , 4.8, 5.1)	2.77	47.6	52.1
$\text{CH}_2\text{--N(2)}$	—	—	—	—	2.48 ( <i>dd</i> , 4.8, 5.1)	2.50	52.8	51.8

**Table 1** continued

<sup>1</sup> H or <sup>13</sup> C location	Compound <b>2c</b> ( $\text{CDCl}_3$ )				Compound <b>2d</b> ( $\text{CDCl}_3$ )			
	$\delta_{\text{H}}\text{-}J(\text{Hz})$ (Exp.)	$\delta_{\text{H}}$ (Calc.)	$\delta_{\text{C}}$ (Exp.)	$\delta_{\text{C}}$ (Calc.)	$\delta_{\text{H}}\text{-}J(\text{Hz})$ (Exp.)	$\delta_{\text{H}}$ (Calc.)	$\delta_{\text{C}}$ (Exp.)	$\delta_{\text{C}}$ (Calc.)
3	—	—	168.7	170.4	—	—	168.8	170.3
5	—	—	174.6	175.3	—	—	174.9	175.8
1'	—	—	118.9	123.3	—	—	119.1	123.9
2'/2''	8.08 ( <i>d</i> , 8.7)	8.40	129.0	133.6	8.10 ( <i>d</i> , 8.7)	8.43	129.1	133.5
3'/3''	6.99 ( <i>d</i> , 8.7)	7.06	114.7	116.6	7.01 ( <i>d</i> , 8.7)	7.04	114.8	116.5
4'	—	—	161.6	166.3	—	—	161.6	166.3
6'	—	—	123.9	128.8	—	—	123.5	128.2
7'/7''	8.18 ( <i>d</i> , 8.4)	8.48	128.0	131.8	8.20 ( <i>d</i> , 8.7)	8.49	128.1	131.5
8'/8''	7.65 ( <i>d</i> , 8.4)	7.86	132.0	135.9	7.71 ( <i>d</i> , 8.7)	7.87	132.1	135.7
9'	—	—	127.0	131.5	—	—	128.1	132.4
10'	—	—	88.9	94.7	—	—	88.2	93.3
11'	—	—	90.1	96.4	—	—	93.7	100.3
12'	—	—	119.6	116.6	—	—	117.3	120.0
13'	8.01 ( <i>s</i> )	8.21	128.8	136.4	7.55 ( <i>d</i> , 8.7)	7.59	128.8	132.1
14'	—	—	138.3	144.0	7.71 ( <i>d</i> , 8.7)	8.00	126.9	130.2
15'	—	—	152.6	157.5	—	—	134.5	137.8
16'	7.04 ( <i>d</i> , 9.0)	6.93	114.4	115.5	—	—	128.3	132.9
17'	7.65 ( <i>d</i> , 9.0)	7.90	137.0	143.5	8.01 ( <i>s</i> )	8.24	131.7	138.0
18'	—	—	—	—	7.12 ( <i>d</i> , 2.4)	7.48	106.6	113.4
19'	—	—	—	—	—	—	158.2	163.4
20'	—	—	—	—	7.18 ( <i>dd</i> , 8.7, 2.4)	7.22	119.9	115.5
21'	—	—	—	—	7.71 ( <i>d</i> , 8.7)	7.99	129.4	134.7
$\text{CH}_3$	0.88 ( <i>t</i> , 6.9)	0.81	14.1	11.4	0.89 ( <i>t</i> , 6.9)	0.90	14.1	9.4
$[\text{OCH}_2]$	4.01/4.11 ( <i>t</i> , 6.6)	3.37/3.56	68.1/69.9	68.5/68.8	4.03/4.09 ( <i>t</i> , 6.6)	3.54/3.69	68.2	68.9
$[\text{CH}_2]$	1.0–2.0	—	22.0–32.0	—	1.0–2.0	—	22.0–32.0	—

<sup>a</sup> The  $R^2$  value would reach 0.9987 if we do not consider contribution of C-9' in the correlation graph

**Fig. 4** **a** COSY spectrum of compound **2b**. **b** NOESY spectrum of compound **2b**



Finally, we directed our attention on compound **2d** which possesses two phenyl rings (A and B) and a naphthalenyl ring (C and D). The naphthalene ring caused slight changes

of the proton and carbon chemical shifts in the ring “B” where H-8', H-8'', and H-7', H-7'' did show downfield shifts of 9.0, and 18.0 Hz, respectively. This change might be

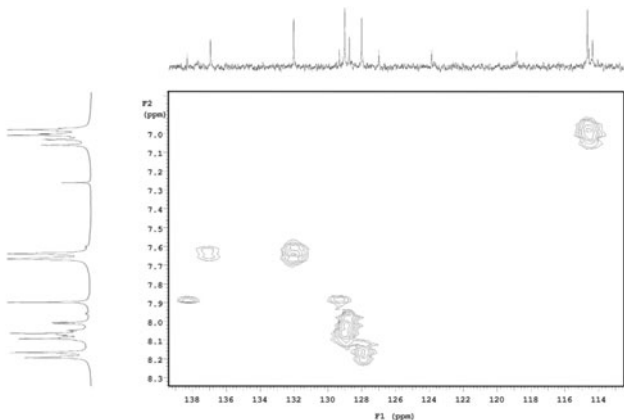


**Fig. 5** HMQC spectrum of compound **2c**

explained considering that the naphthalene ring withdraws electrons a little more than that of the phenyl ring. The acetylenic carbon atoms (C-11' and C-10') also registered lower field shifts of 37.5 and 67.5 Hz in relation with the alkoxyphenyl ring of compound **2a**.

Afterwards, we dedicated our efforts to correctly attribute protons 13', 14', 17', 18', 20', and 21'; and all the 10 carbon nuclei of the naphthyl ring. Both 13' and 17' protons correlated with C-11' as confirmed by HMBC spectrum. COSY spectrum showed that the signal at  $\delta$  7.55 ppm is coupling with another proton at  $\delta$  7.71 ppm, while the proton at  $\delta$  8.01 ppm did not present any coupling with another proton. Therefore, the signals at  $\delta$  7.55 and 8.01 ppm have been assigned to H-13' and H-17', respectively, while the signal at  $\delta$  7.71 ppm is attributed to H-14' (Fig. 6).

In HMQC, the proton at  $\delta$  8.01 ppm correlated with carbon at  $\delta$  131.7 ppm. Thus, the identity of this carbon has been established as C-17'. Similarly, the proton at  $\delta$  7.55 ppm correlated with carbon at  $\delta$  128.8 ppm, indicating clearly that this carbon is C-13'. The assignment of H-14' became complicated due to its superposition with other protons at  $\delta$  7.71 ppm. Both H-13' and H-17' signals

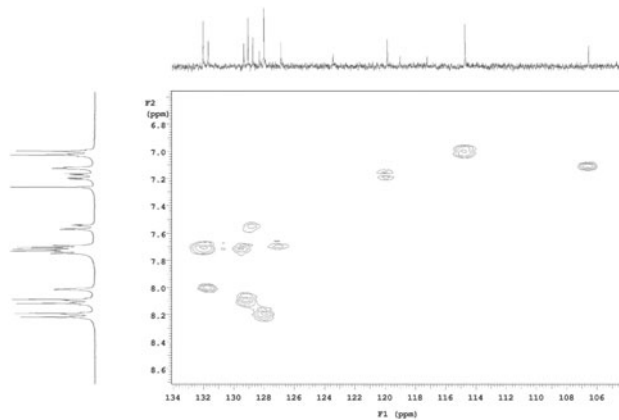


**Fig. 7** HMBC spectrum of compound **2d** depicting the aromatic region

in HMBC spectrum presented coupling with carbon C-15' at  $\delta$  134.5 ppm, thus confirming the attribution of this carbon at 7.71 ppm. The H-17' showed HMBC correlation with the C-21' nucleus at  $\delta$  129.4 ppm. HMQC experiment also verified the location of H-21' at  $\delta$  7.71 ppm. Since this proton at  $\delta$  7.71 ppm in HMBC spectrum showed coupling with carbon at  $\delta$  158.2 ppm, then this carbon must be C-19' (Fig. 7).

COSY spectrum clearly indicated coupling of H-21' at  $\delta$  7.71 ppm with H-20' at  $\delta$  7.18 ppm (Fig. 6). The only hydrogen atom left at  $\delta$  7.12 ppm can, therefore, be assigned as H-18'. Since we confirmed the attribution of H-18' and H-20', it was easy to locate the carbon signals of C-18' and C-20' at  $\delta$  106.6 and 119.9 ppm, respectively, using HMQC spectrum.

This experiment also defined and confirmed the assignment of C-16' at  $\delta$  128.3 ppm. Since, C-20' and C-16' have been verified, the remaining signal at  $\delta$  126.9 ppm should then be C-14'. HMBC spectrum also located the identity of C-21' at  $\delta$  129.4 ppm. The carbon signal at  $\delta$  117.3 ppm can now be assigned as C-12'.

**Fig. 6** **a** Expanded COSY spectrum of compound **2d**. **b** Expanded HMBC spectrum of compound **2d**

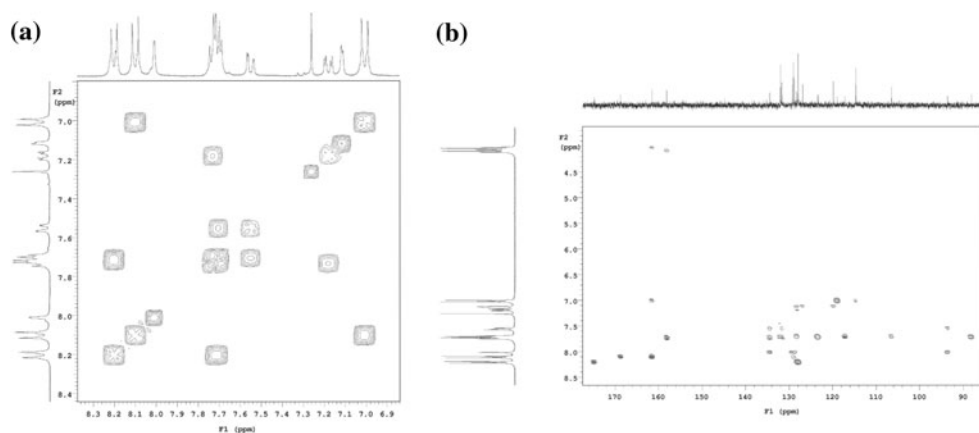


Table 1 shows the assignments of all  $^1\text{H}$  and  $^{13}\text{C}$  NMR signals of compounds **1**, **2a–d**.

#### Geometry optimization

Initially, geometry optimization of compound **1** was carried out using HF/6-31G(d) level of theory employing SDD (including SDD pseudo-potential) for iodine atom because it provides suitable basis set for calculations of molecules containing iodine atom [33]. Since the appearance of  $^1\text{H}$  NMR spectrum of compound **1** exhibited solvent dependence, these calculations have been done with solvent incorporation. In compound **1**, both aromatic rings attached at C-3 and C-5 of the 1,2,4-oxadiazole moiety are co-planar with it. The values of computed bond lengths, bond angles, and dihedral angles are close with the ones described in the literature for 1,2,4-oxadiazole-containing compounds [34–36]. The calculated results with solvent incorporation (either  $\text{CDCl}_3$  or  $\text{C}_6\text{D}_6$ ) are almost the same. Next, we tried to optimize the structures of compounds **2a–d**. The aromatic rings attached to the heterocyclic ring are coplanar in all compounds. This seems reasonable and provides the effective conjugation which is responsible for blue fluorescence (Fig. 8). The phenyl ring C in compound **2b** linked to N-1 of piperazine moiety is disposed equatorially, but the former has rotated to stabilize the conformation. The torsion angle  $\text{C}(14')-\text{C}(15')-\text{N}(1)-\text{C}(18')$ , according to the calculation, turns out to be  $-62.77^\circ$ . The distance between  $\text{H}(14')$  and  $\text{C}(18')$  is  $2.27 \text{ \AA}$  which is close to the sum of Van der Wall radii ( $2.40 \text{ \AA}$ ) between these two atoms. In this way, this part of the molecule, i.e., the rings C and piperazine remain free of any interactions [27].

The nitro group adjacent to the alkoxy function in **2c** did not remain coplanar with ring C, and the oxygen atoms of the former substituent rotated by  $36.32^\circ$  to avoid any interaction with alkoxy moiety. In other words, the nitro group is out-of-the-plane of ring C.

Furthermore, this result is useful to explain the difference between the thermal behavior of compounds **2a** and

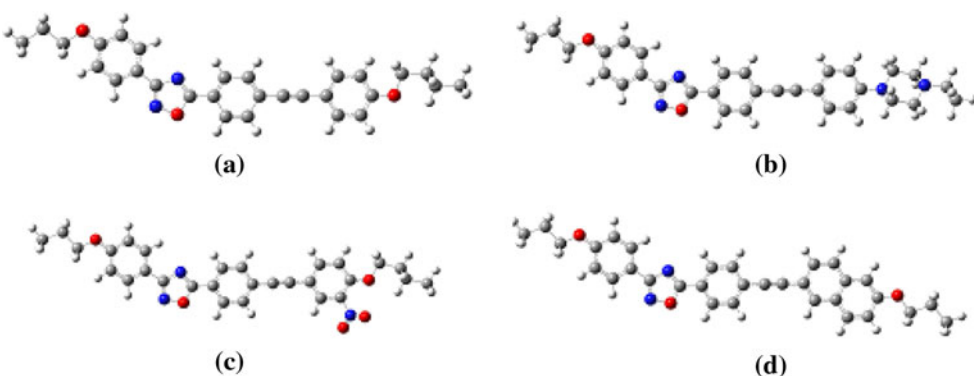
**2c**. According with our earlier publications, the melting point of compound **2a** is  $105^\circ\text{C}$ , while **2c** is  $86^\circ\text{C}$  [22]. With both optimized structures in our hands, we can assume that the melting point decrease in **2c** is due to the non-coplanar arrangement between ring C and the  $-\text{NO}_2$  group. The presence of such group in this position diminishes the intermolecular  $\pi$ -stacking of the conjugated moiety thus lowering the melting point.

#### NMR chemical shift calculations

NMR chemical shift calculations for compound **1** have been carried out by employing DFT B3LYP level theory using SDD (considering SDD pseudo-potential) for I and 6-311++G(d,p) for other atoms including solvent effects. Although all the  $^1\text{H}$  signals obtained by computation are in good agreement with the experimental values, (Table 1) the calculations failed to reproduce the anisotropic effect of the solvent for the aromatic region.

Another interesting point which should be mentioned is that the signals of  $\text{H}-7'$  and  $\text{H}-7''$  as well as  $\text{H}-2'$  and  $\text{H}-2''$  appeared as two doublet pairs in the experimental spectra. On observing the molecular structure of **1**, it is reasonable to rationalize that these protons are in different chemical environments and, therefore, they should have different resonance frequencies. Indeed, our calculations have indicated about this, although their values differ slightly (by about 0.10 ppm only), showing their closeness with the experimental values; therefore, it is difficult to observe them as separate signals in the spectrum. The other possibility is that the observed experimental signal is the sum of the contributions from other conformers present in solution. In order to clarify this point, we have performed the potential energy surface scans followed by the NMR shielding calculations of each rotamer separately. We have started the analysis by fixing the heterocyclic and the aryl rings as coplanar. First, the iodobenzene ring was rotated by an increment of  $30^\circ$  each time and optimized until it reached  $180^\circ$  using HF/6-31G(d) method. The same

**Fig. 8** Optimized structures of compounds **2a–d** at HF/6-31G(d) level



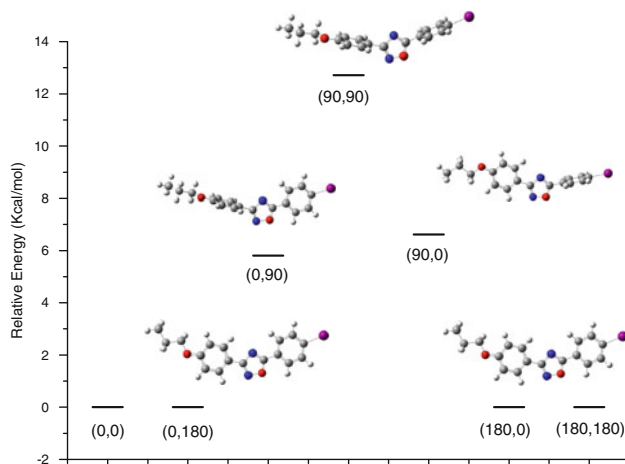


**Fig. 9** Conformational analyses of torsion angles ( $\text{N}4-\text{C}3-\text{C}1'-\text{C}2'$ ,  $\text{N}4-\text{C}5-\text{C}6'-\text{C}7''$ ) calculated using HF/6-31G(d) method

procedure has been carried out for the alkoxyphenyl ring. The conformers of compound **1** along with their relative energies are shown in Fig. 9.

In our conformational analysis of molecule **1**, we found the lowest energy at points 0 and  $180^\circ$  between the oxadiazole and the other aromatic rings. Any deviation of these rings from coplanarity increases the total energy of the molecule and also causes an upfield shift of the aforementioned protons. Thus, it is obvious that when the heterocyclic and iodobenzene rings are coplanar, the

conjugation between them becomes more effective leading to a lower-field shifts of  $\text{H}-7'$  and  $\text{H}-7''$ , respectively. The same occurs with shifts of  $\text{H}-2'$  and  $\text{H}-2''$  when 4-propoxyphenyl ring is rotated. This view is supported by observing the decrease in bond lengths between  $\text{C}_5-\text{C}_6$  and  $\text{C}_1-\text{C}_3$ . Any divergence of the coplanarity of the phenyl rings linked to  $\text{C}3$  and  $\text{C}5$  of the heterocyclic ring increases the just-mentioned bond lengths, and also causes the higher-field proton shifts.

The NMR chemical shift calculations for each conformer separately have been done at B3LYP/6-311++G(d,p) and SDD levels including solvent effects. The computed results of  $^1\text{H}$  chemical shifts for  $7'$  and  $7''$  as well as  $2'$  and  $2''$  protons are summarized in Table 2.

On observing the values from Table 2, it is easy to see that the mean calculated chemical shifts for  $7'$  and  $7''$  as well as for  $2'$  and  $2''$  are closer to the experimental values either in chloroform- $d_3$  or benzene- $d_6$  when the aromatic and heteroaromatic rings are coplanar. The calculations further show that the chemical shifts of  $\text{H}-7'$  and  $\text{H}-7''$  are slightly different, but the difference is too small to be observed in the 300 MHz NMR spectra.

The  $^{13}\text{C}$  computed absorptions are in good agreement with the experimental values with the exception of  $\text{C}-9'$  where the calculated value is  $\delta$  150.1 ppm, and the experimental value is  $\delta$  100.00 ppm. This carbon is exactly the one which is bonded to the iodine atom. Since this atom

**Table 2** Calculated  $^1\text{H}$  chemical shifts for conformers of compound **1**

#### Dihedral plane $\text{N}4-\text{C}5-\text{C}6'-\text{C}7''$

Angle (°)	Chloroform- $d_3$			Benzene- $d_6$		
	$\delta$ $7'$ (ppm)	$\delta$ $7''$ (ppm)	Mean (ppm)	$\delta$ $7'$ (ppm)	$\delta$ $7''$ (ppm)	Mean (ppm)
0	8.171	8.250	8.211	8.098	8.193	8.146
30	7.920	8.058	7.989	7.836	7.999	7.918
60	7.389	7.618	7.504	7.283	7.523	7.403
90	7.264	7.265	7.265	7.148	7.149	7.149
120	7.566	7.426	7.496	7.469	7.320	7.395
150	8.016	7.943	7.980	7.948	7.860	7.904
180	8.250	8.171	8.211	8.193	8.098	8.146

#### Dihedral plane $\text{N}4-\text{C}3-\text{C}1'-\text{N}2'$

Angle (°)	Chloroform			Benzene		
	$\delta$ $2'$ (ppm)	$\delta$ $2''$ (ppm)	Mean (ppm)	$\delta$ $2'$ (ppm)	$\delta$ $2''$ (ppm)	Mean (ppm)
0	8.319	8.444	8.382	8.275	8.402	8.339
30	8.092	8.048	8.070	8.038	7.989	8.014
60	7.688	7.514	7.601	7.607	7.431	7.519
90	7.480	7.397	7.439	7.388	7.291	7.340
120	7.538	7.714	7.626	7.471	7.619	7.545
150	8.063	8.148	8.106	8.025	8.078	8.052
180	8.308	8.427	8.368	8.281	8.366	8.324

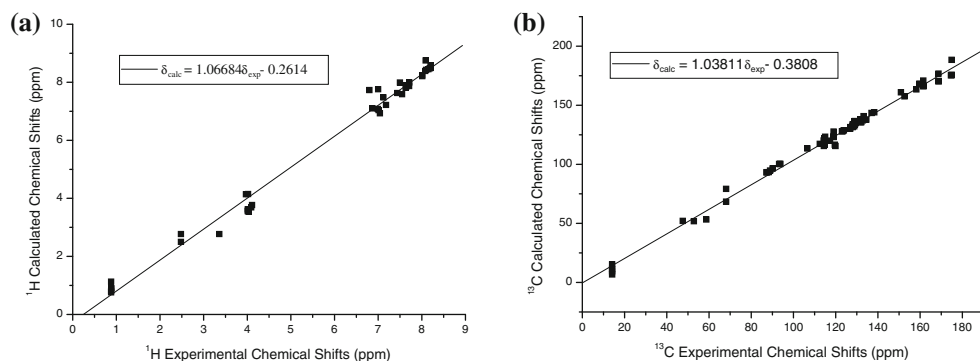


**Fig. 10** **a** Correlation graph of experimental and computed <sup>1</sup>H chemical shifts for compounds **2a–d**. **b** Correlation graph of experimental and computed chemical <sup>13</sup>C shifts for compounds **2a–d**

is voluminous, it is possible that this method is unable to simulate the chemical environment and therefore presents the higher nuclear magnetic shielding for this carbon.

Our results of the DFT–GIAO–PCM calculations for compounds **2a–d** are summarized in Table 1. In order to evaluate the calculations' accuracy, we performed the correlation analysis using the experimental data (Table 1). The correlation graphs presented a linear behavior between the experimental <sup>1</sup>H NMR chemical shifts with the ones predicted theoretically (Fig. 9). It is known that the chemical shifts of protons are more sensitive to solvent, conformations, and physico-chemical parameters [24–31]. It is well documented that GIAO calculations employed for predicting proton signals are, in general, less accurate compared to other nuclei. In this study, we obtained good results in predicting the <sup>1</sup>H chemical shifts of compounds **2a–d**. The computed values for shielding of alkyl and aryl protons are in good agreement with the ones obtained experimentally, where the correlation coefficient ( $R^2$ ) plot is 0.99446 (Table 1). However, the <sup>13</sup>C NMR chemical shifts have been predicted more accurately than those obtained for protons (Fig. 10). Since the carbon atoms are located more internally, it is reasonable to assume that they are less sensitive to solvent effects than protons, hence this discrepancy. The accuracy between the predicted and experimental data has been evaluated by correlation analysis which presented linear behavior including the  $R^2$  value of 0.99639 (Table 1).

## Conclusion

In summary, we have accomplished the complete <sup>1</sup>H and <sup>13</sup>C NMR signal assignments for four 1,2,4-oxadiazoles containing light-emitting liquid crystals. The attributions of the signals have been made by using one- and two-dimensional NMR techniques. Later, we have performed DFT–GIAO (PCM) calculations employing B3LYP/6-311++G(d,p) level of theory for compounds **2a–d**. The

computed shifts were compared with the ones previously assigned using correlation analysis. The predicted values were quite close with the ones obtained experimentally. It is evident from observing the correlation graphs which presented a linear behavior with high  $R^2$  values for both <sup>1</sup>H and <sup>13</sup>C nuclei. Therefore, these calculations also support the signal assignments found experimentally. Finally, the optimized geometry of compounds **2a–d** furnished some structural features which allowed us to clarify some liquid crystal behaviors observed in our earlier studies.

**Acknowledgments** The authors are grateful to the Brazilian National Research Council (CNPq) for financial support. We also thank Dr. R. Longo for helpful discussions. One of the authors, R.A.W.N.F., is thankful to the CNPq for a M.S. fellowship.

## References

1. Vlachos P, Mansoor B, Aldred MP, O'Neill M, Kelly SM (2005) *Chem Commun* 2921
2. O'Neill M, Kelly SM (2003) *Adv Mater* 11:35
3. Hohnholz D, Steinbrecher S, Hanack M (2000) *J Mol Struct* 521:231–237
4. Zhang X-B, Tang B-C, Zhang P, Li M, Tian W-JJ (2007) *J Mol Struct* 846:55
5. Gault JD, Kavanage E, Rodrigues LA, Gallardo H (1986) *J Phys Chem* 9:1860
6. Cristiano R, Gallardo H, Bortoluzzi AJ, Bechtold IH, Campos CEM, Longo RL (2008) *Chem Commun* 5134
7. Attias A-J, Cavalli C, Donnio B, Guillou D, Hapiot P, Malthête J (2002) *Chem Mater* 14:375
8. Shirota YJ (2000) *Mater Chem* 10:1
9. Apreutesei D, Mehl GHJ (2007) *Mater Chem* 17:4711
10. Adachi C, Tsutsui T, Saito S (1989) *Appl Phys Lett* 55:1489
11. Wu F-I, Shu C-F, Chien C-H, Tao Y-T (2005) *Synth Met* 148:133
12. Cha SW, Choi SH, Kim K, Jin J-I (2003) *J Mater Chem* 13:1900
13. Wang C, Jung G-Y, Hua Y, Pearson C, Bryce MR, Petty MC, Batsanov NS, Goeta AE, Howard JAK (2001) *Chem Mater* 13:1167
14. Xu Z, Li Y, Ma X, Gao X, Tian H (2008) *Tetrahedron* 64:1860
15. Han J, Zhang FY, Chen Z, Wang JY, Zhu LR, Pang ML, Meng JB (2008) *Liquid Cryst* 35:1359
16. Han J, Chang XY, Zhu LR, Wang YM, Meng JB, Lai SW, Chui SSY (2008) *Liquid Cryst* 35:1379

17. Gallardo H, Bortoluzzi AJ, Santos DMPD (2008) *Liquid Cryst* 35:719
18. Vieira AA, Cristiano R, Bortoluzzi AJ, Gallardo H (2008) *J Mol Struct* 875:364
19. Vieira AA, Bryk FR, Conte G, Bortoluzzi AJ, Gallardo H (2009) *Tetrahedron Lett* 50:905
20. Cristiano R, Vieira AA, Ely F, Gallardo H (2006) *Liquid Cryst* 33:381
21. Gallardo H, Cristiano R, Vieira AA, Neves RAW, Srivastava RM (2008) *Synthesis* 4:605
22. Gallardo H, Cristiano R, Vieira AA, Filho RAWN, Srivastava RM, Bechtold IH (2008) *Liquid Cryst* 35:857
23. Srivastava RM, Neves RAW, Schneider R, Vieira AA, Gallardo H (2008) *Liquid Cryst* 35:737
24. Bifulco G, Dambruoso P, Gomez-Paloma L, Riccio R (2007) *Chem Rev* 107:3744
25. Bagno A, Saielli G (2007) *Theor Chem Acc* 117:603
26. Alkorta I, Elguero J (1998) *Struct Chem* 9:187
27. Martin NH, Allen NW, Minga EK, Ingrassia ST, Brown JD (1998) *Struct Chem* 9:403
28. Freeman F, Lee K, Hehre WJ (2002) *Struct Chem* 13:149
29. Capriati V, Florio S, Luisi R, Musio B, Alkorta I, Blanco F, Elguero J (2008) *Struct Chem* 19:785
30. Kara I, Kart HH, Kolsuz N, Karakus OO, Deligoz H (2009) *Struct Chem* 20:113
31. Alkorta I, Elguero J (2003) *Struct Chem* 14:377
32. Frisch MJ, Trucks GW, Schlegel HB, Scuseria GE, Robb MA, Cheeseman JR, Montgomery JA Jr., Vreven T, Kudin KN, Burant JC, Millam JM, Iyengar SS, Tomasi J, Barone V, Mennucci B, Cossi M, Scalmani G, Rega N, Petersson GA, Nakatsuji H, Hada M, Ehara M, Toyota K, Fukuda R, Hasegawa J, Ishida M, Nakajima T, Honda Y, Kitao O, Nakai H, Klene M, Li X, Knox JE, Hratchian HP, Cross JB, Adamo C, Jaramillo J, Gomperts R, Stratmann RE, Yazyev O, Austin AJ, Cammi R, Pomelli C, Ochterski JW, Ayala PY, Morokuma K, Voth GA, Salvador P, Dannenberg JJ, Zakrzewski VG, Dapprich S, Daniels AD, Strain MC, Farkas O, Malick DK, Rabuck AD, Raghavachari K, Foresman JB, Ortiz JV, Cui Q, Baboul AG, Clifford S, Cioslowski J, Stefanov BB, Liu G, Liashenko A, Piskorz P, Komaromi I, Martin RL, Fox DJ, Keith T, Al-Laham MA, Peng CY, Nanayakkara A, Challacombe M, Gill PMW, Johnson B, Chen W, Wong MW, Gonzalez C, Pople JA (2003) Gaussian 03, Revision A.1, Gaussian, Inc., Pittsburgh, PA
33. Dunning TH Jr, Hay PJ (1976) In: Schaefer HF III (ed) Modern theoretical chemistry, vol 3. Plenum, New York, pp 1–28
34. Santos SKM, Neves RAW, Bortoluzzi AJ, Srivastava RM (2009) *Acta Crystallogr E* 65:O146
35. Kang SS, Li HL, Zeng HS, Wang HB, Wang PL (2007) *Acta Crystallogr E* 63:O4654
36. Wang PL, Li HL, Kang SS, Zeng HS, Wang HB (2003) *Acta Crystallogr E* 63:O4934